Vibration Based Monitoring Technology for FRP Structures

Sherif Beskhyroun*, Shuichi Mikami**, Tomoyuki Yamazaki***, Toshiyuki Oshima****

*Doctoral Student, Dept. of Civil Eng., Kitami Institute of Technology, (165 Koen-cho, Kitami, 090-8507)
**Associate Professor, Dept. of Civil Eng., Kitami Institute of Technology, (165 Koen-cho, Kitami, 090-8507)
***Research Associate, Dept. of Civil Eng., Kitami Institute of Technology, (165 Koen-cho, Kitami, 090-8507)
****Professor, Dept. of Civil Eng., Kitami Institute of Technology, (165 Koen-cho, Kitami, 090-8507)

In order to detect damage on a structure at an early stage, the health monitoring of structures is studied. In this research, the sensing system, which uses the piezoelectric actuator and the piezoelectric accelerometer, is built and the system is used to detect and locate various types of defects such as bolt release and cracks. The piezoelectric actuator can provide variable excitations in the frequency rang of 0–900 Hz that is effective in measuring a high order mode change associated with the occurrence of damage. In this paper, a damage identification method based on changes in Transfer Function Estimate (TFE) is presented. The method is used to detect damage, predict its location and assess the extent of damage in structures.

Key Words: damage detection, vibration data, health monitoring

1. Introduction

There is a growing need for built-in monitoring systems for civil engineering infrastructures, due to problems such as increasing traffic loads and rising costs of maintenance and repair. In the past two decades, a significant research effort has been directed toward the development of structural health monitoring (SHM) and non-destructive damage detection methods to manage civil structures more efficiently. The term SHM has gained wide acceptance in the past decade as a mean to monitor a structure and provide an early warning of an unsafe condition using real time data. The goal of SHM and other so called 'smart structures' technologies and concepts is to develop 'multifunctional' structures, i.e. structures which provide functionality in other areas besides the primary focus of carrying operational static, dynamic and fatigue loads, with ultimate objective of providing enhanced system level performance. In addition to SHM, a broad range of smart technologies is under development at universities, sensor and actuator companies, and aerospace system manufactures. In recent years, there has been a renewed interest in the damage diagnosis and health monitoring of existing highway bridges using vibration based damage identification techniques. Most vibration-based damage detection theories and practices are formulated based on the assumption that failure or deterioration would primarily affect the stiffness and therefore affect the modal characteristics of the dynamic response of the structure[1-3]. If this kind of changes can be detected and classified, this measure can be further implemented for a bridge monitoring system to indicate the condition, or damage, or remaining capacity of the structures. It can also be used to evaluate the seismic behavior of the structures. Many damage detection schemes rely on analyzing response measurements from sensors placed on the structure[4]. Research efforts have been made to detect structural damage directly from dynamic response measurements in the time domain, e.g. the random decrement technique[5, 6], or from frequency response functions (FRF)[3, 7]. Also, some damage detection methods have been proposed to detect damage using system identification techniques[8]. In this paper, an algorithm based on changes in TFE is presented. The algorithm is used to detect damage, locate its position and monitor the increase in damage using only the measured data without the need for any modal identification or

numerical models. The method is applied to the experimental data extracted from a bridge model after inducing some defects to its members.

2. Theoretical description

Let $P_{xy}(f)$ denote the TFE, relating two time histories, x(t) and y(t). The absolute difference in absolute TFE before and after damage can then be defined as

$$\Delta_{xy}(f) = \left\| P_{xy}(f) \right| - \left| P^{*}_{xy}(f) \right\| \quad (1)$$

where $P_{xy}(f)$ and $P_{xy}^{*}(f)$ represent the TFE of the undamaged and damaged structures respectively. When the change in TFE is measured at different frequencies on the measurement range from f_1 to f_m, a matrix $[\Pi_r]$ can be formulated as follows

$$\Pi_r = \begin{bmatrix} \Delta_{1r}(f_1) & \Delta_{1r}(f_2) & \ldots\ldots & \Delta_{1r}(f_m) \\ \Delta_{2r}(f_1) & \Delta_{2r}(f_2) & \ldots\ldots & \Delta_{2r}(f_m) \\ . & . & \ldots\ldots & . \\ . & . & \ldots\ldots & . \\ . & . & \ldots\ldots & . \\ \Delta_{nr}(f_1) & \Delta_{nr}(f_2) & \ldots\ldots & \Delta_{nr}(f_m) \end{bmatrix}_r \quad (2)$$

where n represents the number of measuring points and r represents the number of reference channel. In matrix $[\Pi_r]$, every column represents the changes in TFE at different measuring channels but at the same frequency value. Each measuring channel will be used as a reference for the other channels ($r = 1 : n$). Therefore, the matrix $[\Pi_r]$ will be formulated n different times (3D matrix). The summation of TFE changes over different frequencies using different references can be used as the indicator of damage occurrence. In other words, the first damage indicator is calculated from the sum of rows of each matrix, $[\Pi_r]$ and then summing up these changes over different references

$$Total\_Change = \sum_r \begin{Bmatrix} \sum_f \Delta_{1r}(f) \\ \sum_f \Delta_{2r}(f) \\ . \\ . \\ . \\ \sum_f \Delta_{nr}(f) \end{Bmatrix}_r \quad (3)$$

where $f = f_1 : f_m$ and $r = 1 : n$.

This indicator is used to detect the damage; however, it was found to be a weak indicator of damage localization. A statistical decision making procedure is employed to determine the location of damage. The first step in this procedure is the picking of the maximum change in TFE at each frequency value (the maximum value in each column of matrix $[\Pi_r]$) and discarding all other changes in TFE measured at other nodes. For example in matrix $[\Pi_r]$ (Eq. 2), if $\Delta_{3r}(f_1)$ is the maximum value in the first column then this value will be used as $B_{3r}(f_1)$ and other values in this column will be discarded. The same process is applied to the different columns in matrix $[\Pi_r]$ to formulate the matrix of maximum changes of TFE at different frequencies, $[B_r]$. It should be noted that $[B_r]$ is a 3D matrix where each value of r ($r = 1 : n$) formulates one matrix

$$B_r = \begin{bmatrix} 0 & 0 & 0 & .. & 0 \\ 0 & B_{2r}(f_2) & 0 & .. & 0 \\ B_{3r}(f_1) & 0 & 0 & .. & B_{3r}(f_m) \\ 0 & 0 & B_{4r}(f_3) & .. & 0 \\ . & . & . & .. & . \\ . & . & . & .. & . \\ 0 & 0 & 0 & .. & 0 \end{bmatrix}_r \quad (4)$$

In order to monitor the frequency of damage detection at any node, a new matrix $[E_r]$ is formulated. The matrix consists of 0's at the undamaged locations and 1's at the damaged locations. For example in the matrix $[E_r]$, we put a value of 1 corresponding to the locations of $B_{3r}(f_1)$, $B_{2r}(f_2)$ and so on, as shown in the following expression

$$E_r = \begin{bmatrix} 0 & 0 & 0 & \ldots\ldots & 0 \\ 0 & 1 & 0 & \ldots\ldots & 0 \\ 1 & 0 & 0 & \ldots\ldots & 1 \\ 0 & 0 & 1 & \ldots\ldots & 0 \\ . & . & . & \ldots\ldots & . \\ . & . & . & \ldots\ldots & . \\ 0 & 0 & 0 & \ldots\ldots & 0 \end{bmatrix}_r . \quad (5)$$

The total of maximum changes in TFE is calculated from the sum of the rows of matrix $[B_r]$ using different references. At each value of r, the sum of rows of matrix $[B_r]$ will result in one vector. Therefore, n different vectors can be obtained. The sum of these vectors is stored in one vector $\{Z\}$;

$$Z = \sum_r \begin{Bmatrix} \sum_f B_{1r}(f) \\ \sum_f B_{2r}(f) \\ . \\ . \\ . \\ \sum_f B_{nr}(f) \end{Bmatrix}_r . \quad (6)$$

Similar to the previous procedures, the total number of times of detecting the damage at different nodes is calculated from matrix $[E_r]$ as

$$K = \sum_r \begin{Bmatrix} \sum_f E_{1r}(f) \\ \sum_f E_{2r}(f) \\ . \\ . \\ . \\ \sum_f E_{nr}(f) \end{Bmatrix}_r . \quad (7)$$

In order to reduce the effect of noise or measurement errors, a value of two times standard deviation of the elements in vector {K} will be subtracted from the vector {K}. Any resulting negative values will be removed. The same procedures is applied to the vector {Z} as follows

$$T = \begin{Bmatrix} Z_1 - 2\sigma \\ Z_2 - 2\sigma \\ . \\ . \\ . \\ Z_n - 2\sigma \end{Bmatrix} \quad (8)$$

where $\sigma = \sqrt{\sum_{i=1}^{n} (Z_i - \overline{Z})^2} \Big/ (n-1)$, $\overline{Z} = \sum_{i=1}^{n} Z_i \Big/ n$,

$$I = \begin{Bmatrix} K_1 - 2\beta \\ K_2 - 2\beta \\ . \\ . \\ . \\ K_n - 2\beta \end{Bmatrix} \quad (9)$$

where $\beta = \sqrt{\sum_{i=1}^{n} (K_i - \overline{K})^2} \Big/ (n-1)$, $\overline{K} = \sum_{i=1}^{n} K_i \Big/ n$.

The first damage location indicator is defined as the scalar product of { T } and { I } as shown in the following expression

$$Dam\_Ind\_1 = \begin{Bmatrix} T_1 \times I_1 \\ T_2 \times I_2 \\ . \\ . \\ . \\ T_n \times I_n \end{Bmatrix} . \quad (10)$$

Another damage location indicator is formulated as follows: the sum of rows of matrix $[B_r]$ at each reference channel represents a column in the following matrix

$$\Psi = \begin{bmatrix} \sum_f B_{11}(f) & \sum_f B_{12}(f) & ..... & \sum_f B_{1n}(f) \\ \sum_f B_{21}(f) & \sum_f B_{22}(f) & ..... & \sum_f B_{2n}(f) \\ . & . & ..... & . \\ . & . & ..... & . \\ . & . & ..... & . \\ \sum_f B_{n1}(f) & \sum_f B_{n2}(f) & ..... & \sum_f B_{nn}(f) \end{bmatrix} \quad (11)$$

where the first subscript represents the channel number and the second represents the reference number. A process of choosing the maximum value at each column and discarding other values of that column is used to construct the matrix Ψ_{max}.

$$\Psi_{max} = \begin{bmatrix} 0 & \sum_f B_{12}(f) & .. & 0 \\ \sum_f B_{21}(f) & 0 & .. & \sum_f B_{2n}(f) \\ . & . & .. & . \\ . & . & .. & . \\ . & . & .. & . \\ 0 & 0 & .. & 0 \end{bmatrix} \quad (12)$$

A new matrix [N] is constructed from 1's corresponding to the values in matrix Ψ_{max} and 0's at other locations as

$$N = \begin{bmatrix} 0 & 1 & . & . & . & 0 \\ 1 & 0 & . & . & . & 1 \\ . & . & . & . & . & . \\ . & . & . & . & . & . \\ . & . & . & . & . & . \\ 0 & 0 & . & . & . & 0 \end{bmatrix} . \quad (13)$$

The sum of rows of matrix [Ψ_{max}] defines the vector { Ψ_{sum} }

$$\Psi_{sum} = \sum_r \Psi_{max} , \quad (14)$$

and the sum of rows of matrix N defines the vector { N_{sum} }

$$N_{sum} = \sum_r N . \quad (15)$$

Then the second damage location indicator is defined as the scalar product of vectors { Ψ_{sum} } and { N_{sum} }

$$Dam\_Ind\_2 = \Psi_{sum} . \times N_{sum} . \quad (16)$$

Damage indicators 1 and 2 will be used to determine the damage location. On the other hand, the total change in TFE will be used to detect the occurrence of damage and assess the damage extent.

3. FRP beam

The change in natural frequency due to the occurrence of damage has been examined using the experimental data that was obtained from FRP beam. The basic dimensions of the beam and the positions of actuator and accelerometers are shown in Fig. 1. The actuator force acts on the vertical direction. Channel 1 trough 3 measure the response of the flange in the vertical direction and channel 4 measures the acceleration response of the web in the horizontal direction. The damage was introduced to the beam by reducing the torque in one bolt in the left support of the beam. The torque in the undamaged state equals 90N. The torque is reduced in one bolt to 60N, 30N and 0N. No significant changes in the resonant frequencies were observed in any damage case. Fig. 2 shows Power Spectral Density (PSD) at the different channel before and after reducing the torque to 0N. In this figure, it is clearly indicated that the change in resonant frequencies are very small even after releasing one bolt completely.

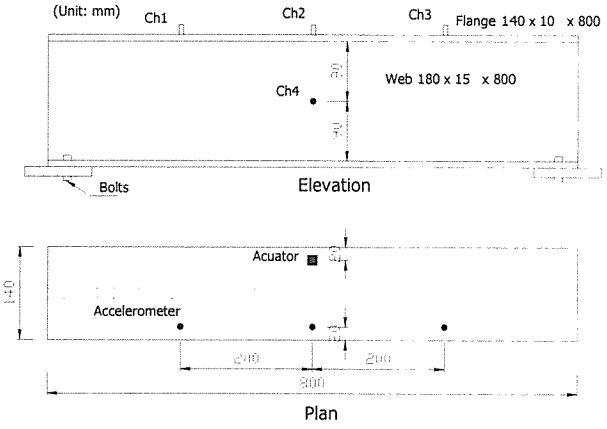

Fig. 1 Basic dimensions of the FRP beam

4. Bridge model

4.1 Experimental setup and equipment

In this research, a bridge model is examined after inducing damage with different levels to some members. The model consists of two girders and six cross beams. Each cross beam is connected to the girders with four bolts; two bolts in each side. The model dimensions and layout are shown in Figs. 3 and 4. The multi-layer piezoelectric actuator is used for local excitation. The main advantage of using piezoelectric actuator is that it produces vibration with different frequencies ranging from 0 to 900 Hz that is effective in exciting different mode shapes[9), 10)]. Five natural frequencies are measured in the range of the excitation frequency (from 0 to 400 Hz) at 43.75, 118.85, 212.5, 300, 393.75 Hz. The actuator force amplitude is 0.2 kN. The actuator is located at the center of the upper flange of the main girder (Figs. 3 and 4). The location of the actuator is not changed during different damage states of the structure. The effects of changing the actuator location on the accuracy of the results are not studied in this research. The excitation forces used for the undamaged and damaged structure are random, equal in amplitude and have the same vibration waveform but the excitation force does not need to be measured. One accelerometer is mounted at the bottom of each cross beam to measure the acceleration response in the vertical direction at the mid span of each cross beam, as shown in Fig. 4. Seven cases of damage are introduced to the specimen as follows:

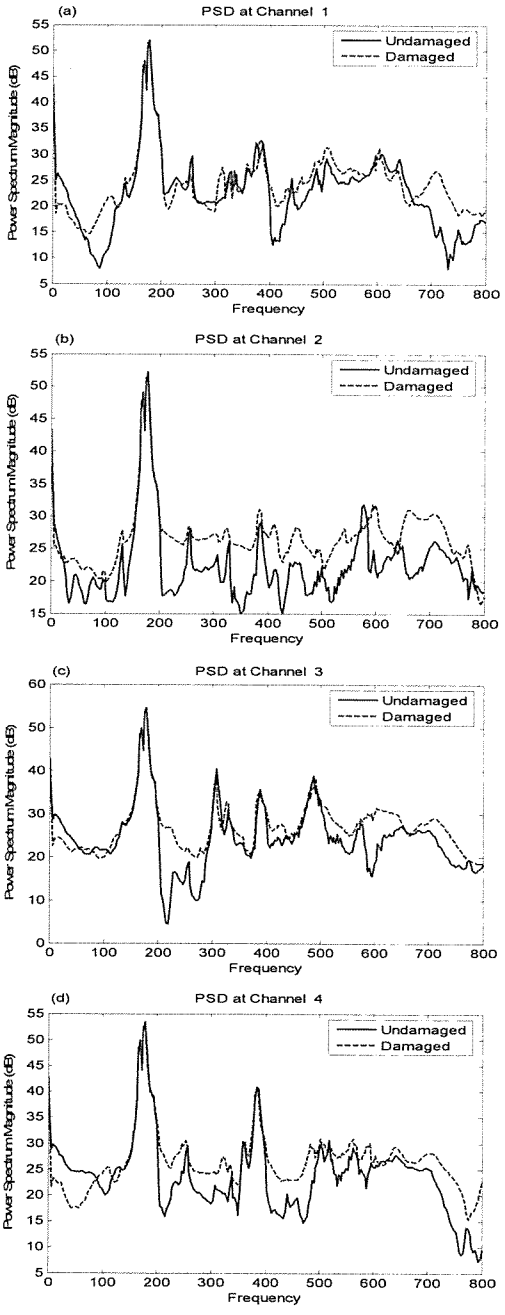

Fig. 2 Power Spectral Density at different channels

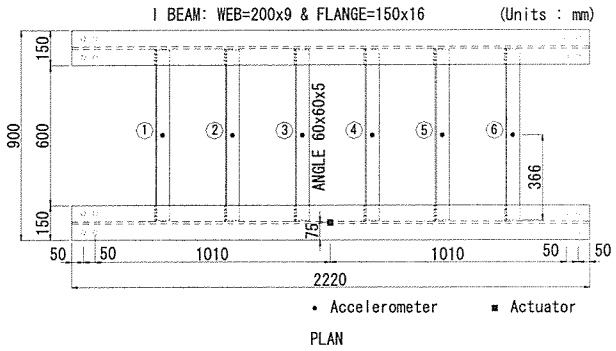

Fig. 3 Basic dimensions of the bridge model

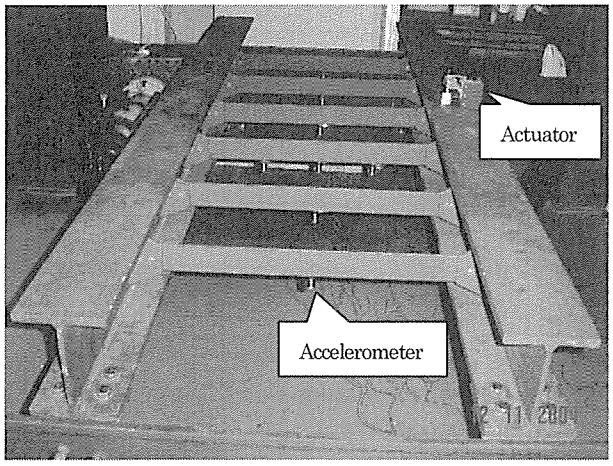

Fig. 4 Accelerometers and actuator positions

Case 1: Removing one bolt completely from the left side of cross beam no.

Case 2: Case 1 + releasing one bolt at the left side of cross beam no. 2.

Case 3: Case 2 + removing one bolt at the right side of cross beam no. 2.

Case 4: Case 3 + releasing one bolt at the right side of cross beam no. 2.

Case 5: Removing one bolt from the left side of cross beam no. 3.

Case 6: Removing one bolt from the left side of cross beam no. 2. The same damage is introduced to cross beam no. 5.

Case 7: A torch cut of 10 mm length and 1 mm width is introduced at the middle of cross beam no. 2. The cut starts from the edge of the horizontal plate of the beam.

4.2 Damage identification algorithm applied to different damage cases for the bridge model

(1) Before introducing any damage

One of the drawbacks of vibration based damage identification methods is that these methods sometimes produce false positive readings due to noise, measurement errors or environmental changes. It is therefore very important to determine if the results obtained from any damage identification method are due to damage or due to other changes. Because of this need, the experiment was performed a number of times on the undamaged structure prior to the introduction of any damage. TFE data for two different sets of data obtained from the undamaged structure is shown in Fig. 5. Small changes in TFE can be observed in this figure, obviously due to noise and measurement errors. TFE data in the frequency range of 5–800 Hz was used for the proposed method. The total change in TFE was determined using Eq. (3) and the results are shown in Fig. 6. The total change in TFE ranged from about 800 to 1200 dB. When the total change of TFE was determined using other sets of data that were obtained from the undamaged structure, similar and very close values of the total change in TFE were obtained. The total change of TFE will be used as an indicator of damage detection and damage increase. On the other hand, damage indicators 1 and 2 will be used to identify the damage location.

(2) Cases 1, 2, 3 and 4 (damage at beam no. 2)

The accuracy of the damage identification methods based on FRF or cross spectral density (CSD) is dependent on the frequency range in which FRF[3] or CSD[10] is measured. The accuracy of the damage identification methods based on mode shapes is dependent on which mode shapes are used. The accuracy of the results is sometimes reduced when some of the used mode shapes have nodes at the damage location[2]. In order to overcome this problem, it was decided to use TFE magnitudes in the frequency range of 5–800 Hz in the proposed algorithm. This range of measurement covers most of the total measurement range of TFE data (from 1 to 800 Hz). The resulting damage indicators for damage case 1 are plotted in Fig. 7. In Fig. 7 (a), the total change in TFE (Eq. 3) increased at all channels after removing the first bolt. The total change in TFE due to the removal of one bolt is much larger than that due to noise and measurement errors (Fig. 6). Although the maximum total change of TFE is observed at channel 2 (the damage location), the total change in TFE is not always a good indicator of damage location. Damage indicators 1 and 2 have determined the damage location at channel 2 accurately, as shown in Figs. 7 (b), (c), respectively. After increasing the damage level in beam no. 2, the same previous remarks were also observed. The total changes in TFE (Eq. 3) for the four cases of damage and for the intact structure are plotted in Fig. 8. The following remarks can be drawn from this figure:

- The total change in TFE due to noise is less than 1200 dB at all channels with close values at the

different channels.

- After removing the first bolt (Case 1), the total change in TFE increased slightly at the undamaged locations (damage at one location will change the overall stiffness of the structure) and increased remarkably at the damaged location (channel 2).
- After releasing one more bolt (Case 2), the total change in TFE continued to increase slightly at the undamaged locations and remarkably at the damaged location.
- After introducing damage to the third and fourth bolts (Cases 3 and 4), the total change in TFE increased slightly at the damaged location since the beam has already lost most of its stiffness after removing the second bolt.

Therefore, it can be concluded that the total change in TFE can be used to monitor the increase in damage successfully.

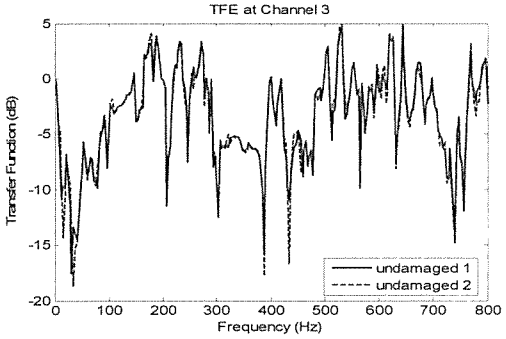

Fig. 5 TFE for two tests performed on the undamaged structure

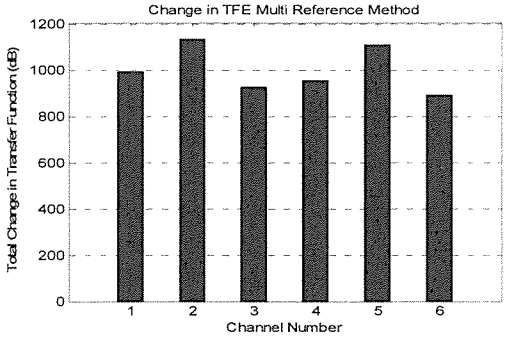

Fig. 6 Total change in TFE due to noise

(3) Case 5 (damage at beam no. 3)

The accuracy of damage identification methods based on mode shapes is sometimes reduced when the damage exists at the node of the used modes. Therefore, the damage position is changed in this case to examine the effects of changing the damage position. The TFE magnitude is measured in the frequency range of 5–800 Hz. The results of this case are shown in Fig. 9. Damage indicator 1 has detected the damage at channel 3 with some false positive readings appearing at other channels

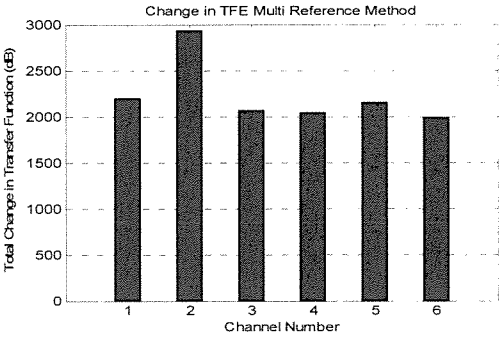

Fig. 7 (a) Total change in TFE

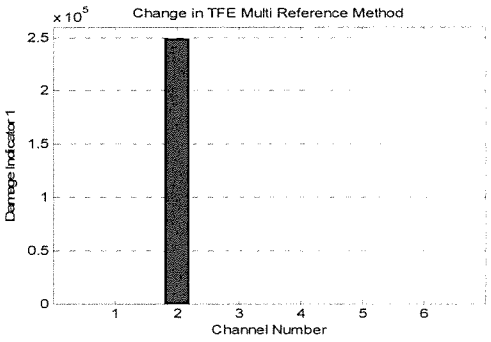

Fig. 7 (b) Damage localization using damage indicator 1

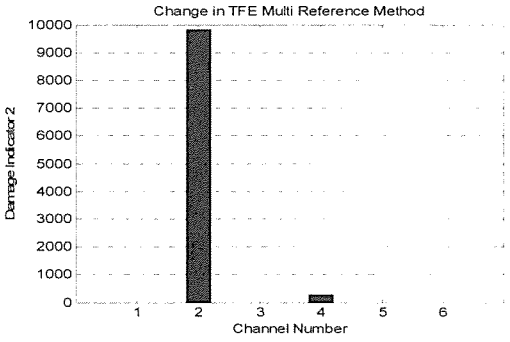

Fig. 7 (c) Damage localization using damage indicator 2

Fig. 7 Proposed algorithm results for damage case 1

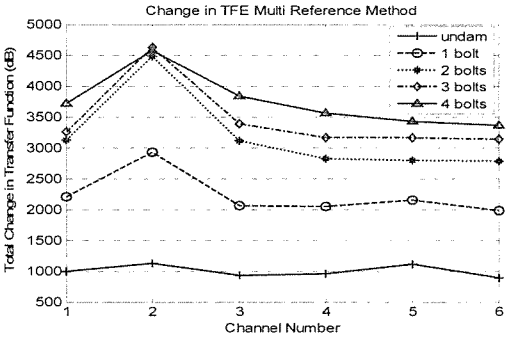

Fig. 8 Total change in TFE for different damage cases at beam no. 2

(undamaged locations), as shown in Fig. 9 (a). On the other hand, damage indicator 2 has detected the damage accurately without any readings at the undamaged locations Fig. 9 (b). Damage indicator 2 performed better for this case than damage indicator 1.

(4) Case 6 (damage at beams no. 2 and 5)

This case is introduced to investigate the feasibility of the algorithm to detect multiple-damage. The TFE magnitude is measured in the frequency range of 5–800 Hz. Damage at the two positions is detected and localized accurately with no false positive readings using damage indicators 1 and 2, as shown in Figs. 10 (a), (b). As indicated in these figures, damage indicators values at channel 2 is higher than that at channel 5. This difference is because the structure is not exactly symmetrical, the fixation of the bolts in the two angles (2 and 5) is not exactly the same and the amount of noise or measurement errors stored in the data of each measuring channel is not equal.

(5) Case 7 (crack at beams no. 2)

Case 7 is introduced to investigate the feasibility of the algorithm to detect different types of damages. The TFE magnitude is measured in the same frequency range of 5–800 Hz. In Fig. 11 (a), damage indicator 1 could not identify the damage location accurately in this case, although the maximum value of this indicator exists at channel 2 (damage location). On the other hand, damage at channel 2 is detected and localized accurately with no false positive readings using damage indicator 2, as shown in Fig. 11 (b). It was noticed that the total change in TFE for this case was smaller than the case of removing one bolt (Case 1), which means that detecting the damage in this case was more difficult than the case of bolt release. This is because the effect of removing any bolt on the vibration response of the beam is greater than the case of localized crack. When the method was applied to detect a crack length of 20 mm at same location of this case, both damage indicators identified the damage more accurately.

5. Conclusions

Changes in the TFE magnitude due to the presence of structural damage have been investigated. The experimental results obtained from a bridge model demonstrate the usefulness of the changes in TFE magnitude as a diagnostic parameter in detecting the damage, locating its position and monitoring the increase in damage. The main advantages of the proposed methods are:

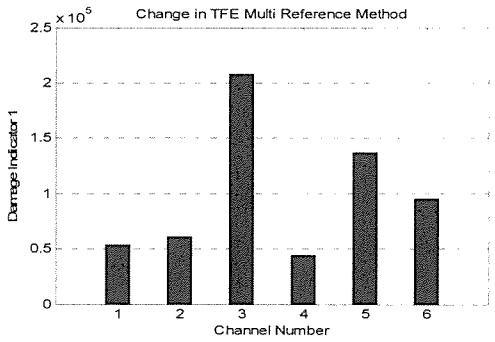

Fig. 9 (a) Damage localization using damage indicator 1

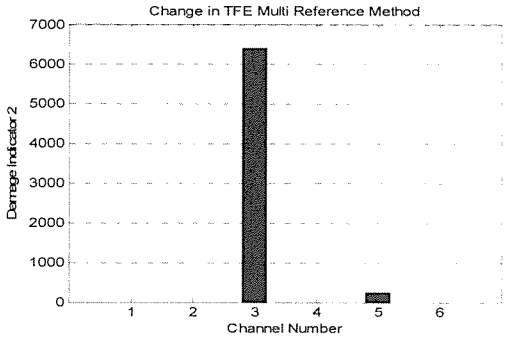

Fig. 9 (b) Damage localization using damage indicator 2

Fig. 9 Proposed algorithm results for damage case 5

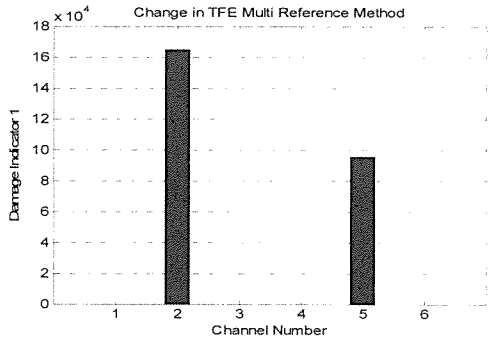

Fig. 10 (a) Damage localization using damage indicator 1

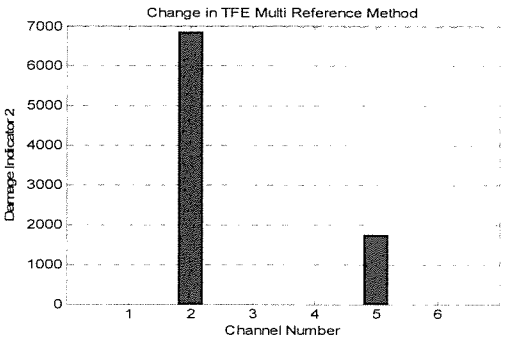

Fig. 10 (b) Damage localization using damage indicator 2

Fig. 10 Proposed algorithm results for damage case 6

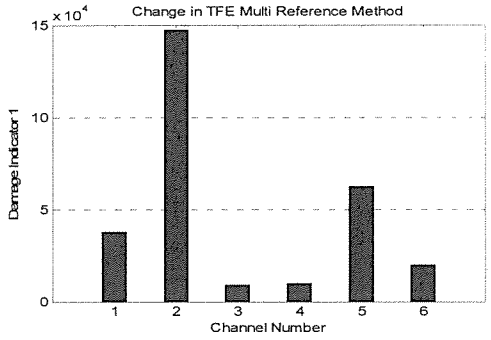

Fig. 11 (a) Damage localization using damage indicator 1

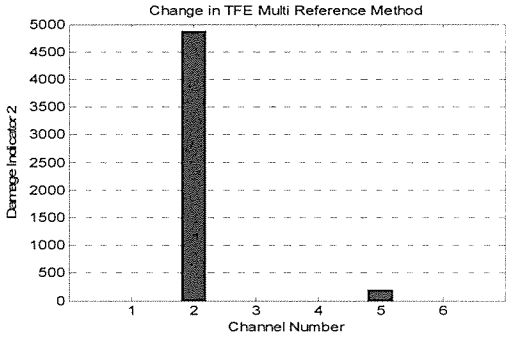

Fig. 11 (b) Damage localization using damage indicator 2

Fig. 11 Proposed algorithm results for damage case 7

(1) High accuracy in detecting and locating small damage.

(2) The proposed method encompasses the first three steps of the process of damage detection – existence, localization and monitoring the damage increase being based on only the measured data without the need for any modal identification.

(3) The accuracy of damage identification methods based on changes in mode shapes are sometimes reduced when the damage occurs at a node of the used mode shapes. And, the accuracy of damage identification methods based on changes in FRF or CSD are dependent on the measurement range in which FRF or CSD are measured. The proposed method overcomes this drawback by using TFE data in the total measured frequency range.

(4) Vibration based damage identification methods sometimes produce false positive readings due to measurement errors, noise and environmental changes. The proposed method has shown better results in identifying the changes in TFE associated with damage from the changes attributed to noise or measurement errors.

Acknowledgement

This research is supported by the Grant-in-Aids for Scientific Research, Ministry of Education. The authors wish to express their gratitude for this support.

References

1) Doebling S. W., C. R. Farrar, M. B. Prime, and D. W. Shevitz, *Damage Identification and Health Monitoring of Structural and Mechanical Systems from Changes in their Vibration Characteristics*, A Literature Review, Los Alamos National Laboratory Report, LA-13070- MS, 1996.

2) Farrar C. R. and D. A. Jauregui, *Damage Detection Algorithms Applied to Experimental and Numerical Model Data from the I-40 Bridge*, Los Alamos National Laboratory Report, LA-12979-MS, 1996.

3) Sampaio R. P. C., Maia N. M. M. and Silva J. M. M., Damage detection using the frequency response function curvature method, *Journal of Sound and Vibration*, 226(5), pp. 1029-1042, 1999.

4) Peeters B., Maeck J. and De Roeck G., Vibration-based damage detection in civil engineering: excitation sources and temperature effects, *Smart Materials and Structures*, 10, pp.518-527, 2001.

5) E. Kummer, J. C. S. Yang and N. G. Dagalakis, Detection of fatigue cracks in structural members, *2nd American Society of Civil Engineering/EMD Specialty Conference*, Atlanta, Georgia, 445-460, 1981.

6) J. C. S. Yang, J. Chen and N. G. Dagalakis, Damage detection in offshore structures by the random decrement technique, *Journal of Energy Resources Technology*, American Society of Mechanical Engineers 106, 38-42, 1984.

7) R. G. Flesch and K. Kernichler, Bridge inspection by dynamic tests and calculations dynamic investigations of Lavent bridge, *workshop on Structural Safety Evaluation Based on System Identification Approaches* (H. G. Natke and J. T. P. Yao, editors), 433-459, Lambrecht/ Pfalz, Germany: Vieweg & Sons, 1988.

8) H. G. Natke and J. T. P. Yao, System identification methods for fault detection and diagnosis, *International Conference on Structural Safety and Reliability*, American Society of Civil Engineers, New York, 1387-1393, 1990,

9) Oshima T. et al., Study on damage evaluation of joint in steel member by using local vibration excitation, (In Japanese), *Journal of Applied Mechanics JSCE*, Vol.5, pp.837-846, 2002.

10) Beskhyroun S., Mikami S., Oshima T. and Yamazaki T., Modified damage identification algorithm based on vibration measurements, *Journal of Applied Mechanics, JSCE*, Vol.7, pp. 97-107, 2004.